Malaysian Journal of Chemistry, 2026, Vol. 28(1), 481-489
(Special Issue: *12th International Conference of the College of Science & 3rd Conference of Chemistry Department 2025*)

Facile Method to Prepare TiO_2 and CuO/TiO_2 Heterojunction and its Investigation for MB Degradation

Aseel Adnan Ouda[1]* and Firas Kamil Mohamad[2]
[1]Ministry of Education, Educational Directorate of Holy Kerbala, Kerbala, Iraq
[2]University of Kerbala, Department of Physics, College of Science, Kerbala, Iraq
*Corresponding author (e-mail: aseeladnanalobaidi@gmail.com)

High-purity TiO_2 and CuO/TiO_2 nanocomposite systems were prepared via a simple polyol solvothermal method. The synthetic precursors for nanomaterials were titanium isopropoxide (TTIP) and copper nitrate trihydrate. Several characteristic techniques, including X-ray diffraction (XRD), field-emission scanning electron microscopy (FESEM), energy-dispersive X-ray spectroscopy (EDX), Fourier transform infrared (FTIR) spectroscopy, Brunauer-Emmett-Teller (BET) testing, and photoluminescence (PL) spectroscopy, were employed to investigate the as-synthesised nanomaterials. The findings showed that the undoped TiO_2 and CuO/TiO_2 composite samples exhibited a rice-like structure after heat treatment for 3 hours at 450 °C in an oven. The optimized MB degradation reached approximately 99.87% at 160 min, compared to bare TiO_2 nanoparticles, which achieved approximately 93.81% after 180 min of UV irradiation.

Keywords: Polyol method, rise-like, photodegradation, CuO, heterojunction

Received: September 2025; Accepted: November 2025

Chemicals used in daily living, such as dyes in wastewater, have recently emerged as a new source of environmental contamination. Furthermore, it can alter the human body and affect organisms, as a small amount of dye can cause poisoning [1]. Researchers have developed numerous techniques to remove such dyes from water [2, 3]. Photocatalysis is an efficient and environmentally friendly method for removing pollutants, such as dyes, from water compared to other methods. One of the most used semiconductor photocatalysts, titanium dioxide (TiO_2), is distinguished by its non-toxicity, corrosion resistance, chemical stability, low cost, and thermal resilience [4, 5]. There are numerous applications for TiO_2 nanomaterials, such as photocatalysis and environmental purification [6, 7], self-cleaning surfaces [8, 9], solar energy and electronics [10, 11], cosmetics and skin protection [12]. Due to the main limitation of TiO_2, which is a semiconductor material (n-type) with a broad band energy gap of approximately 3.2 eV. Many studies have suggested several techniques to enhance the photocatalytic efficacy of TiO_2 in the ultraviolet (UV) spectrum, including doping [13], semiconductor combination [14], and surface modification [15]. Among these techniques, TiO_2 is combined with another semiconductor (p-type) with a narrow band gap, forming a heterojunction [16]. A heterojunction system is a medium composed of two distinct materials with different energy gaps on either side of the junction. One heterojunction-based structure is a metal oxide system comprising two semiconductors. Copper(II) oxide (CuO) is a small-band-gap semiconductor (1.2-1.5 eV), making it a suitable catalyst for various applications, such as photocatalytic removal of organic pollutants [17, 18]. The formation of a CuO/TiO_2 heterojunction is occasioned by the excitation of the electron (e) from the valence band (VB) to the conductive band (CB) of CuO and its transfer to the conductive band of the TiO_2 [19, 20].

This study aimed to prepare pure TiO_2 and CuO/TiO_2 heterojunctions using a polyol-mediated solvothermal method, which was subsequently tested as photocatalysts for the elimination of the organic pollutant methylene blue (MB). This method provides precise control over material properties, such as shape, particle size, and dispersion, by using a polyol solvent, such as ethylene glycol (EG), which stabilizes metal ions and promotes uniform particle growth. The suggested preparation approach is expected to facilitate the formation of a stable heterojunction, enhancing the photocatalytic efficiency of the produced materials and promoting efficient electron-hole pair separation.

EXPERIMENTAL

Materials

Titanium isopropoxide ($C_{12}H_{28}O_4Ti$, TTIP), ethylene glycol ($C_2H_6O_2$), cupric nitrate trihydrate ($Cu(NO_3)_2$ $3H_2O$), high-purity water, absolute ethanol (C_2H_5OH), ammonium hydroxide solution (NH_4OH), and methylene blue (MB) were purchased from the local market in Baghdad, Iraq. Every reagent was analytical grade and utilized without additional purification.

Preparation of TiO_2 and CuO/TiO_2 Heterojunction

Pristin TiO_2 and CuO/TiO_2 heterojunction system was prepared via a simple polyol-mediated solvothermal

†Paper presented at the 12th International Conference of the College of Science & 3rd Conference of Chemistry Dept. 2025

process [21]. First, 100 mL of solvent was placed in a reactor and warmed up to 170 °C using a hot plate and magnetic stirring. Next, 2.5 mL of titania precursor TTIP was added dropwise to the EG solvent. A white titanium complex glycolate precipitate was obtained after mixing. The mixing process was maintained at a constant stirrer rate for 5 hours. After the mixing period was completed, the mixture was left to cool down gradually to room temperature. The resulting titanium complex glycolate was then cleaned with absolute ethanol and deionized water several times to remove impurities from the mixture. Finally, the obtained white nano powders were dried in an oven at 80 °C for 6 hours and then annealed for 3 hours at 450 °C.

To synthesize the CuO/TiO_2 heterojunction system, after the white titanium solution was formed and cooled to room temperature, 0.25 g of the copper precursor was dissolved in 5 mL of absolute ethanol and then added to the solution. A few drops of NH_4OH solution were added to reach a pH value of 6. The resulting solution was then reheated to 170 °C and stirred for an additional hour at a constant rate. Finally, the obtained mixture was centrifuged and repeatedly cleaned with ethanol and high-purity water. The prepared CuO/TiO_2 heterojunction was dried at 80 °C for 8 hours and then annealed at 450 °C for 3 hours.

Characterization Methods

The crystalline phase of the prepared samples was determined using X-ray diffraction (XRD) analysis (Aeris, Panalytical, Holland). XRD analysis was performed with Cu Kα irradiation (α =1.541 Å). The prepared samples were scanned at (Δ2θ =0.05°/s) over a range of 5°-90° to form the XRD patterns. To determine the sample morphology, a Field Emission Scanning Electron Microscopy (FESEM) model Inspect F50 (USA) was used, coupled with an energy-dispersive X-ray (EDX) analyser. The EDX technique was used to detect the chemical elements in the sample structure. Fourier transform infrared spectrometry (FTIR) (Shimadzu, 8400s, Japan) was used to determine the functional groups of TiO_2 and the CuO/TiO_2 nanocomposite using the KBr pressed disc method. To determine the surface area, size, and volume of pores in the TiO_2 and CuO/TiO_2 metal oxide systems, a low-temperature nitrogen adsorption analysis using a Brunauer-Emmett-Teller (BET) analyser (Micromeritics ASAP 2010) was employed. The surface area was determined from adsorption data at relative pressures (p/p_0) between 0.05 and 0.3. The PL studies of the prepared sample were conducted using a PL spectrophotometer (SHIMADZU RF5301, Japan) in the wavelength range 300-850 nm.

Photocatalytic Test

To assess the photocatalytic activity of the prepared TiO_2 and CuO/TiO_2 binary systems, MB dye photodegradation was performed under UV irradiation. The UV source is equipped with a 16 W power supply. A 500 mL MB solution at 10 ppm was placed in a vessel. Then, 150 mg of the photocatalyst was added to the solution. The mixture was magnetically agitated in the dark for at least 1 hour. This step was to establish the adsorption-desorption equilibrium of MB on the catalyst and to remove inaccuracies from elementary absorption. At the end of the dark period, about 3 mL was withdrawn to determine the dye concentration. This was taken as the primary concentration (C_o). Then, the MB solution was irradiated with UV light. Samples of approximately 3 mL were collected every 20 minutes to monitor the decreasing MB concentration as it degraded. The photocatalyst was separated from the solution by centrifuging for 5 minutes at 4000 rpm. The MB concentration (C_t) in the supernatant was then measured. Finally, the resulting clean solution was analyzed by UV-Vis spectroscopy (Shimadzu, 1900i-Japan) in the 190–1100 nm wavelength region to monitor MB degradation in the final solution.

RESULTS AND DISCUSSIONS

Figure 1 shows the XRD pattern of the reference sample TiO2 and the CuO/TiO_2 heterojunction system prepared by the polyol-mediated solvothermal method. The diffraction pattern for undoped TiO_2, as shown in the Figure, displays characteristic bands for the anatase crystal phase (JCPDS No. 21-1272). No other diffraction peaks appear, indicating a high-purity phase structure for the TiO_2 photocatalyst. The observed crystalline planes, (101), (004), (200), (105), (204), (220), (215), and (224), occur in the anatase TiO_2 sample. These correspond to diffraction angles (2θ) at 25.3°, 37.8°, 48.0°, 55.1°, 62.7°, 70.3°, 75.1°, and 82.7°, respectively.

The XRD result of the TiO_2 sample modified with CuO nanoparticles (as a heterojunction) provided a pattern similar to that of bare anatase TiO_2 nanoparticles without any additional diffraction peaks. Moreover, the results showed that the peak intensity decreased and broadened as CuO was doped into the TiO_2 nanoparticles. This finding is due to the Ti^{4+} substitutional ions being replaced by Cu^{2+} dopant ions, which prevented the lattice nanostructure from distorting. The Debye-Scherrer equation was used to determine the average crystalline size of the obtained nanostructure:

$$D = 0.9\lambda/\beta \quad (1)$$

where D is the size of the crystal particle, k is a constant usually 0.9, λ is the X-ray wavelength (1.541 Å), β is the value of the full diffraction peak width at half maximum, and θ is the peak diffraction angle. The results show that the CuO/TiO_2 heterojunction system has a lower average crystallite size of approximately 5.72 nm compared to the pristine TiO_2 nanoparticles, which have an average crystallite size of approximately 7.5 nm.

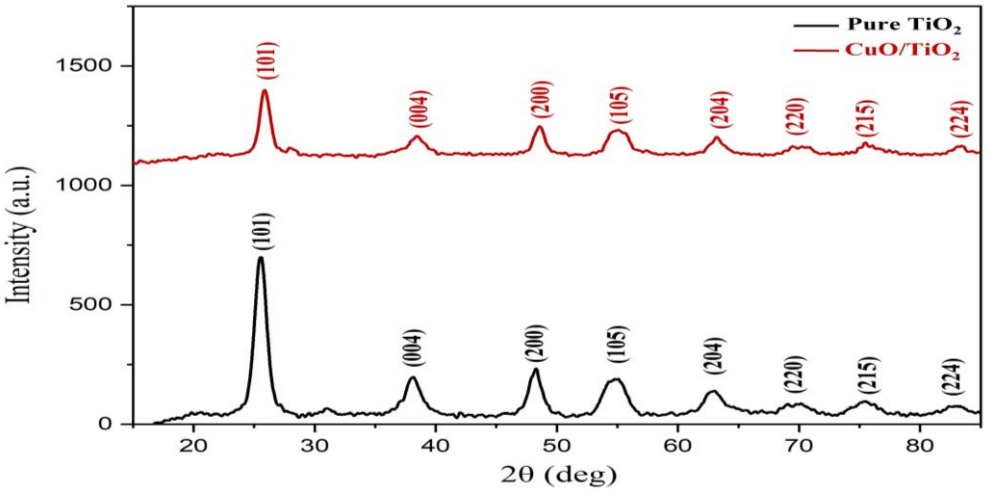

Figure 1. XRD diffraction pattern of TiO_2 and CuO/TiO_2 heterojunction system.

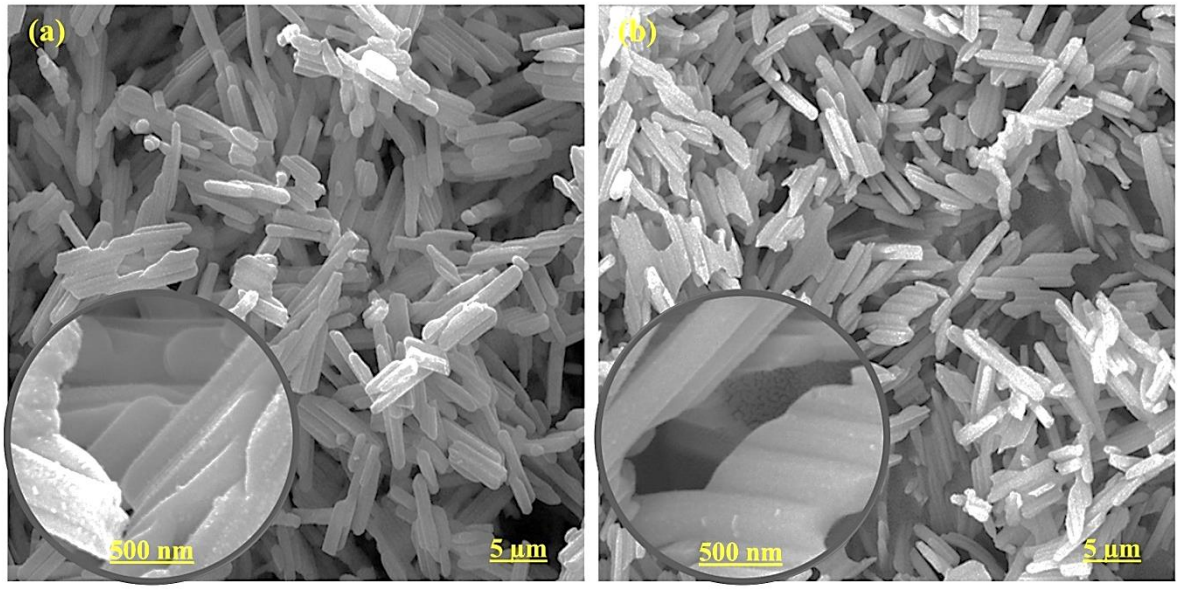

Figure 2. FESEM images of (a) TiO_2 nanoparticles and (b) CuO/TiO_2 heterojunction.

FESEM was used to investigate the morphologies of pristine anatase TiO_2 and the CuO/TiO_2 heterojunction. The results showed that both undoped TiO_2 and the CuO/TiO_2 metal oxide system exhibit regular one-dimensional structures. No notable changes could be shown in the morphology of the TiO_2 and CuO/TiO_2 oxide nanostructures, as observed in Figure 2 (a) and (b). It can be confirmed that Cu^{2+} nanoparticles inserted into TiO_2 did not further alter its lattice structure. The particles of undoped TiO_2 formed aggregates with a one-dimensional rice-like structure, with an average length and diameter of approximately 3171.36 nm and 417.81 nm, respectively. Due to the ionic radii of Cu^{2+} (0.73 Å) being larger compared to Ti^{4+} (0.61Å), the CuO/TiO_2 heterojunction was observed, with an average length of approximately 2521.31 nm, and an average diameter of 389.58 nm.

Figures 3(a) and (b) show the EDX results of bare TiO_2 and CuO/TiO_2 heterojunction. The results indicated the presence of peaks for titanium (Ti), oxygen (O), and copper (Cu), as well as a small amount of precarious carbon (C). The carbon peak is attributed to the tape used to hold the sample during the measurement.

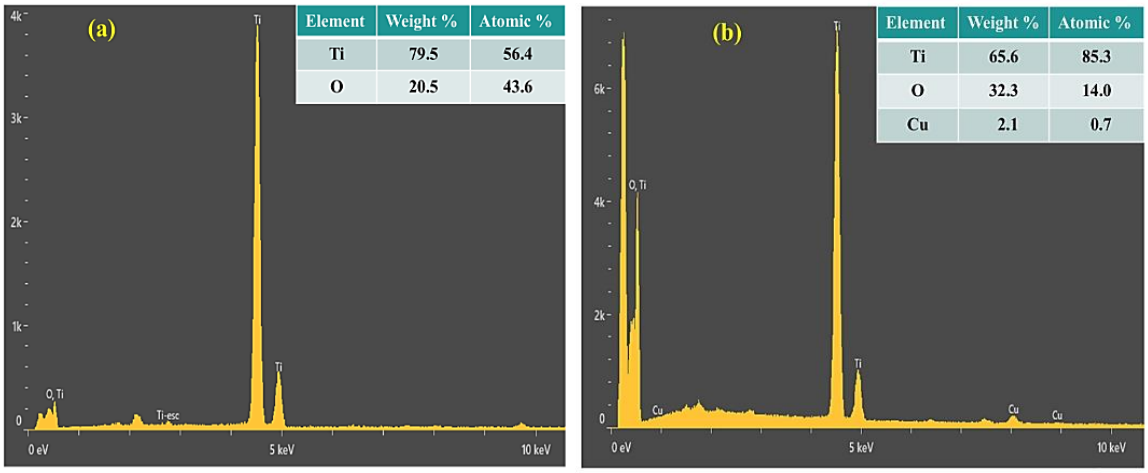

Figure 3. EDX spectrum of (a) undoped TiO_2 and (b) CuO/TiO_2 heterojunction.

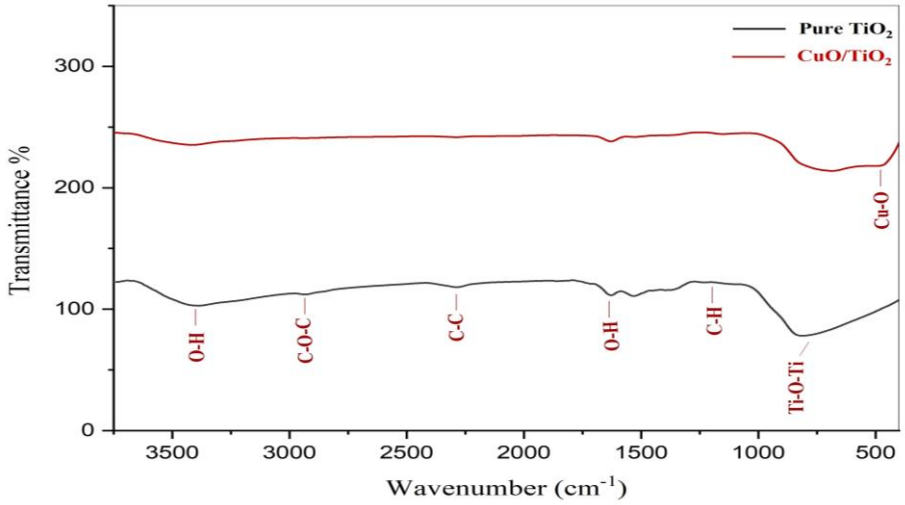

Figure 4. FTIR spectrum of pristine TiO_2 and CuO/TiO_2 heterojunction.

The FTIR spectrum of the undoped TiO_2 and modified CuO/TiO_2 heterojunction is clarified in Figure 4. The broad absorption band at about 3400 cm^{-1} and a weaker peak at 1618 cm^{-1} were assigned to the O-H stretching vibration of absorbed water molecules [22]. At 2281 cm^{-1}, a weaker stretching band in the spectrum corresponded to the C-C band. While the peak at 2930 cm^{-1} was assigned to the C-O-C bond [23]. The peak observed below 900 cm^{-1} in the FTIR spectrum was attributed to the stretching mode of the Ti-O-Ti bond [24]. Therefore, the peak at 770 cm^{-1} indicated the formation of the TiO_2 lattice network. The peaks observed at 480 cm^{-1}, 521 cm^{-1}, and 596 cm^{-1} were referred to the stretching vibration form of Cu-O [18].

Figure 5 (a) and (b) display nitrogen (N_2) adsorption and desorption isotherms as well as the pore volume distribution curve (insert) of pure TiO_2 and CuO/TiO_2 heterojunction. The N_2 isotherms displayed a type IV isotherm with an H3 hysteresis loop according to the IUPAC classification [25]. The BET isotherms and pore-size distribution curves indicated a mesoporous nanostructure. The specific surface area and the average pore diameter of pure TiO_2 were 78.76 m^2/g, and the particle size was 7.50 nm, respectively. The surface area and average pore diameter of the CuO/TiO_2 heterojunction nanorise are approximately 32.07 m^2/g and 8.53 nm, respectively. The measurements show that the surface area of the as-prepared CuO/TiO_2 nanocomposite was remarkably smaller than that of undoped TiO_2, but the pore diameter became larger. This finding indicated that CuO doping enhanced the phase evolution of TiO_2.

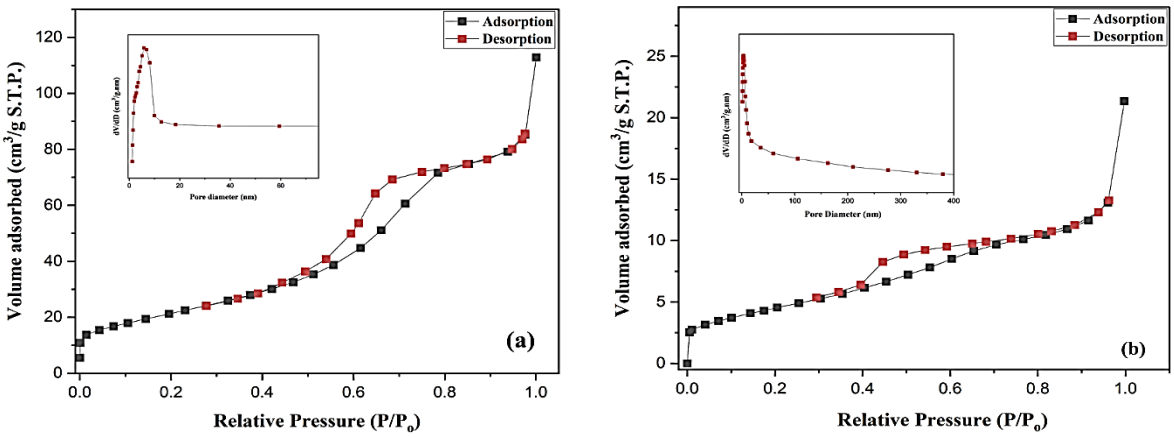

Figure 5. N_2 adsorption isotherms of undoped TiO_2 and CuO/TiO_2 heterojunction.

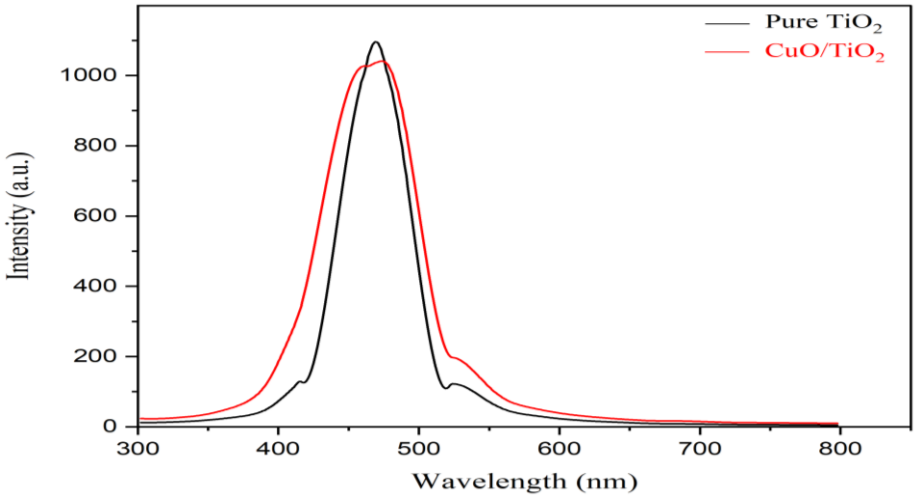

Figure 6. PL spectra of bare TiO_2 and CuO/TiO_2 heterojunction.

Photoluminescence spectroscopy is used to determine the fate of electron-hole pairs in a semiconductor and to estimate the trapping rate of charge carriers [26]. The emission peaks in PL spectra are principally associated with the oxygen defects and excitons created by the addition of copper oxide [27]. The emission peak occurred at approximately 465 nm, possibly due to the band-to-band transition of photoelectrons in TiO_2, leading to the creation of self-trapped excitons, as shown in Figure 6. The emission intensity decreased when the TiO_2 sample was doped with CuO. The excited electron may leap to the newly formed defect level in CuO rather than from the valence band (VB) to the conduction band (CB) of TiO_2, thereby lowering the recombination rate. Moreover, CuO nanoparticles promote the formation of shallow trap centers and increase the concentration of oxygen vacancies at charged grain boundaries. The vacancies in oxygen resist the movement of electrons that are not trapped in the defect centers. As a result, these electrons and holes cannot recombine, thereby increasing photocatalytic activity.

The improvement in the photocatalytic behaviour of broad-band-gap TiO_2 semiconductors by forming heterojunctions with narrow-band-gap semiconductors, such as CuO, has been extensively investigated [28-30]. When CuO nanoparticles grow on the surface of the TiO_2 matrix, the photoresponse of TiO_2 is extended into the visible spectrum [31]. Since the TiO_2 conduction band (CB) is more positive than the CuO conduction band, photogenerated electron injection is anticipated to occur from the band gap of CuO nanoparticles into the TiO_2 conduction band, while holes may accumulate in the valence band (VB) of CuO to form hole centres [32], as shown in Figure 7. The photoexcited electron-hole pairs produced can convert water molecules on CuO/TiO_2 catalysts into OH^- ions and H^+ cations. Adsorbed OH^-

ions can be oxidized by forming hydroxyl radicals ($OH^{\bullet}$) through a reaction with accumulating holes in the CuO valence band. Superoxide radical anion ($O_2^{\bullet-}$) is created when concentrated electrons in the TiO_2 conduction band move to oxygen atoms that have been adsorbed on the surface of TiO_2.

Additionally, the adsorbed oxygen (O_2) atoms may react with H^+ cations to generate an adsorbed hydroperoxyl radical (HO_2), which then reacts with H^+ and an electron to generate Hydrogen peroxide (H_2O_2). Then, H_2O_2 can reduce to hydroxyl radicals when it reacts with a single peroxide radical anion [33]. The quantity of $OH^{\bullet}$ and $O_2^{\bullet-}$ radicals primarily regulates the breakdown kinetics of a specific concentration of an organic molecule, such as methylene blue (MB), into carbon dioxide (CO_2), water (H_2O), and harmless products [34].

The photocatalytic reactions of interest in MB degradation are explained in the following equations under ultraviolet (UV) irradiation:

$$CuO/TiO_2 + h\nu\ (UV) \rightarrow CuO/TiO_2\ (e^- + h^+) \quad (2)$$

$$H_2O \leftrightarrow H^+ + OH^- \quad (3)$$

$$OH^- + h^+ \rightarrow OH^{\bullet} \quad (4)$$

$$O_2 + e^- \rightarrow O_2^{\bullet-} \quad (5)$$

$$O_2 + H^+ \rightarrow HO_2^{\bullet} \quad (6)$$

$$H_2O + h^+ \rightarrow OH^{\bullet} + H^+ \quad (7)$$

$$HO_2^{\bullet} + e^- + H^+ \rightarrow H_2O_2 \quad (8)$$

$$H_2O_2 + O_2^{\bullet-} \rightarrow 2^{\bullet}OH \quad (9)$$

$$Dye + OH^{\bullet}/\ O_2^{\bullet-} \rightarrow CO_2 + H_2O + \text{harmless products} \quad (10)$$

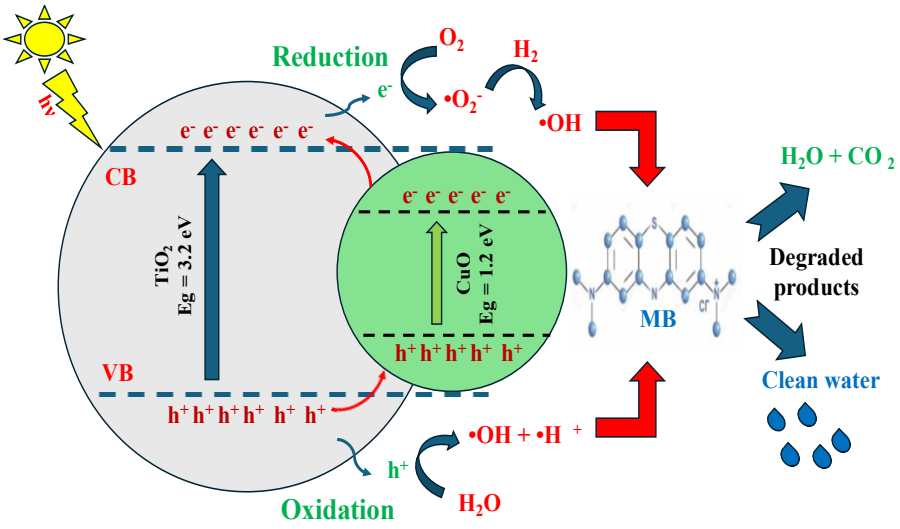

Figure 7. Schematic diagram of charge transfer on the TiO_2 surface modified CuO nanoparticles.

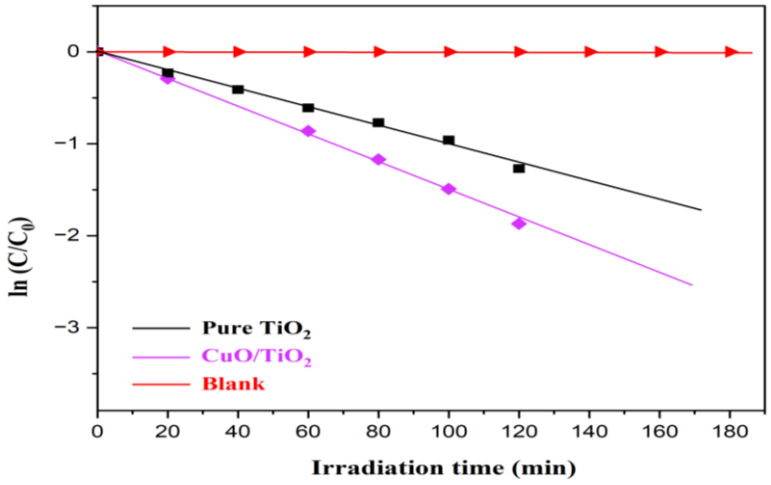

Figure 8. First-order kinetics constant for the MB degradation on the prepared photocatalysts, pure TiO_2, CuO/TiO_2 heterojunction under UV irradiation, and in the dark (blank) without irradiation.

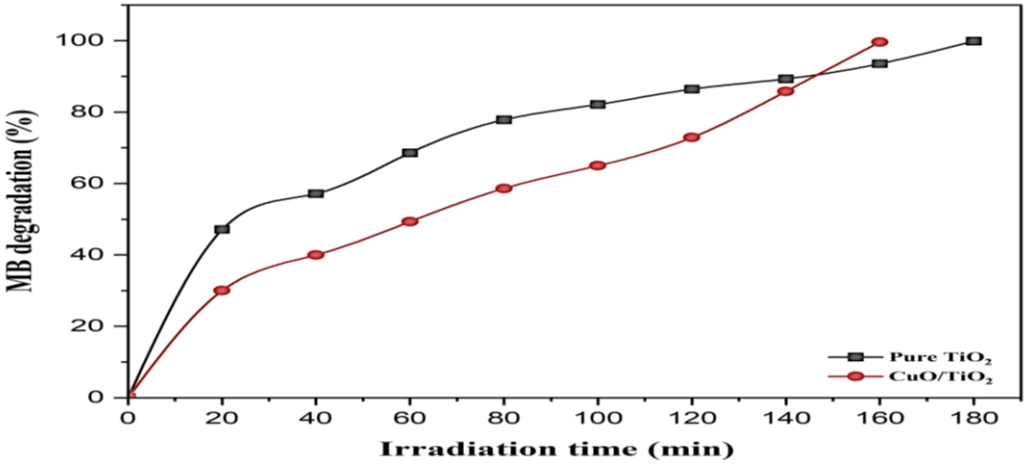

Figure 9. MB degradation efficiency versus UV irradiation time of undoped TiO_2 and CuO/TiO_2 heterojunction.

Figure 8 showed that the photocatalytic elimination of MB dye corresponds to a pseudo-first-order formula, which computes the photodegradation rate constant noted as (k) [35]:

$$\ln (C/C_o) = -kt \quad (11)$$

where C_o is the original MB concentration, C is the concentration at a selected time, and k is the first-order photodegradation rate constant. The resulting linear recession coefficients (R^2) were comparatively high, suggesting that MB photodegradation follows the Langmuir-Hinshelwood kinetic style. The finding indicated that the rate constant of undoped TiO_2 increased with the presence of CuO nanoparticles in its nanostructure. The kinetic constant (k) of pure TiO_2 was about 0.0102 min^{-1}, while it was about 0.0152 min^{-1} for CuO/TiO_2 heterojunction.

Figure 9 explained the MB dye degradation efficiency as a function of UV illumination time for undoped TiO_2 and CuO/TiO_2 samples. The as-prepared pristine TiO_2 rise-like structure showed an MB degradation ratio of approximately 93.57% in solution after 180 minutes. In contrast, the CuO/TiO_2 heterojunction shows about 99.64% after 160 minutes of irradiation. Since the CuO is confined to the structure of the TiO_2, there will be an enhancement for the restricted electron to recombine with a hole and increase the photocatalytic activity.

CONCLUSION

In this paper, the TiO_2 and CuO-doped TiO_2 heterojunction samples were successfully prepared using the polyol solvothermal method. The characterization techniques revealed the formation of a high-purity anatase phase with a rice-shaped morphology. The average length of undoped TiO_2 and CuO/TiO_2 catalysts was about 3171.36 nm and 2521.31 nm, respectively. A higher photocatalytic activity for MB degradation was observed with the as-prepared CuO/TiO_2 heterostructure, achieving about 99.64% under UV irradiation. This improvement was due to Cu^{2+} coupling within the TiO_2 structure, which inhibits electron-hole recombination and thereby enhances photocatalytic performance. Therefore, a more efficient heterojunction photocatalyst can be used to treat other organic pollutants in water under visible-light irradiation.

CONFLICT OF INTEREST

The authors declare that there is no conflict of interest regarding the publication of this paper.

ACKNOWLEDGEMENTS

The authors would like to express their sincere gratitude to the Department of Physical Sciences, Nanotechnology Laboratory, University of Kerbala, for providing the laboratory facilities and valuable support during this research.

REFERENCES

1. Lin, J., Ye, W., Xie, M., Seo, D. H., Luo, J., Wan, Y., and Bruggen, B. V. D. (2023). Environmental impacts and remediation of dye-containing wastewater. *Nature Reviews Earth and Environment*, **4**, 785–803.

2. Dutta, S., Gupta, B., Srivastava, S. K., and Gupta, A. K. (2021). Recent advances on the removal of dyes from wastewater using various adsorbents: A critical review. *Materials Advances*, **2**, 4497–4531.

3. Nayeri, D. and Mousavi, S. A. (2020) Dye removal from water and wastewater by nanosized metal

oxides-modified activated carbon: A review on recent researches. *Journal of Environmental Health Science and Engineering*, **18**, 1671–1689.

4. Nagaraj, K., Radha, S., Deepa, C. G., Raja, K., Umapathy, V., Badgujar, N. P., Parekh, N. M., Manimegalai, T., Devi, L. A., and Uthra, C. (2025) Photocatalytic advancements and applications of titanium dioxide (TiO_2). *Next Research*, **2**, 100180.

5. Sharma, R., Prakash, J. (2025). TiO2 Nanomaterials: Synthesis, Properties, Modifications, and Applications. In *Titanium Dioxide-Based Multifunctional Hybrid Nanomaterials: Application on Health, Energy and Environment*, *Cham: Springer Nature Switzerland*, 1–25.

6. Haghighi, P., Haghighat, F. (2024) TiO_2-based photocatalytic oxidation for indoor air VOCs removal: A review. *Building and Environment*, **249**, 111108.

7. Rashid, R., Shafiq, I., Gilani, M. R. H. S., Maaz, M., Akhter, P., Hussain, M., Jeong, K. E., Kwon, E. E., Bae, S., and Park, Y. K. (2024). Advancements in TiO_2-based photocatalysis for environmental remediation. *Chemosphere*, **349**, 140703.

8. Besleaga, C., Tomulescu, A. G., Zgura, I., Stepanova, A., Galca, A. C., Laafar, S., Zorila, F. L., Alexandru, M., Pintilie, I., and Iliescu, M. (2024). Reticulated mesoporous TiO_2 scaffold for self-cleaning surfaces. *Ceramics International*, **50**, 42264–42275.

9. Mallia, J., Anastasi, A., and Briffa, S. (2023). Developing self-cleaning photocatalytic TiO_2 nanocomposite coatings. *International Journal of Surface Engineering and Interdisciplinary Materials Science*, **11**, 1–20.

10. Gao, J., Wang, S., Cai, H., Chen, S., Zheng, L., Li, Y., and He, G. (2025). Portable photocatalytic fuel cell with anatase/rutile TiO_2 heterophase junction. *International Journal of Hydrogen Energy*, **97**, 259–269.

11. Kadhim, N., Harouni, M., and Hachim, D. (2025). Improving Solar Cell Performance with TiO_2/PVA Nanocoating and Natural Dyes from Acacia and Spirulina, 1–20.

12. Berardinelli, A. and Parisi, F. (2021) TiO_2 in the food industry and cosmetics. In *Titanium Dioxide (TiO_2) and its Applications*, *Elsevier*, 353-371.

13. Unal, F., Ok, S., Unal, M., Topal, S., Cellat, K. and Şen, F. (2020). Transition-metal-doped TiO_2 photoelectrodes for dye-sensitized solar cells. *Journal of Molecular Liquids*, **299**, 112177.

14. Erfan, N., Mahmoud, M., Kim, H., and Barakat, N. (2023). Synergistic doping to overcome electron–hole recombination in TiO_2 photocatalysis. *Frontiers in Chemistry*, **11**, 1301172.

15. Hu, W., Yang, S., and Yang, S. (2020) Surface modification of TiO_2 for perovskite solar cells. *Trends in Chemistry*, **2**, 148–162.

16. Panepinto, A., Krumpmann, A., Cornil, D., Cornil, J., and Snyders, R. (2021) Switching TiO_2 conductivity via ion implantation. *Applied Surface Science*, **563**, 150274.

17. Nazim, M., Khan, P., Asiri, M., and Kim, H. (2021). Rapid photocatalytic degradation with porous CuO nanosheets. *ACS Omega*, **6**, 2601–2612.

18. Islam, R., Saiduzzaman, M., Nishat, S., Kabir, A., and Farhad, S. (2021). Ce-doped CuO nanoparticles: photocatalysis and DFT+U. *Colloids and Surfaces A*, **617**, 126386.

19. Phongsapatcharamon, T. (2020) CuO-decorated TiO_2 NT heterojunction photodetector, 1–14.

20. Sun, A., Zhao, Y., Li, J., Lai, H., Li, H., Yang, Z., He, J., Pan, P., and Zhang, R. (2025). Visible-light degradation of PET using CuO/TiO_2. *Vacuum*, **240**, 114602.

21. Alosfur, F., Ouda, A., Ridha, N., and Abud, H. (2019). High photocatalytic activity of TiO_2 nanorods. *Materials Research Express*, **6**, 065028.

22. Kotov, N., Keskitalo, M. and Johnson, M. (2025) Nano-FTIR spectroscopy of liquid water. *Spectrochimica Acta Part A*, **330**, 125640.

23. Baloguna, S., Oyesholab, H., Belloa, S., and Ojoa, S. (2024). Ixora coccinea extract for green synthesis of TiO_2 nanoparticles. *Journal of Materials Engineering*, **2**, 279–287.

24. Vidales, M., Caudana, A., Mauricio, R., Méndez, G., Caballero, F., and Mendoza, A. (2021) FTIR studies of titanium butoxide sol–gel transitions. *Journal of Sol-Gel Science and Technology*, **99**, 315–325.

25. Medrano, B., Celis, N., and Giraldo, I. (2022) Nitrogen adsorption–desorption isotherm analysis of aluminosilicates, 1–48.

26. Li, Q., Anpo, M., You, J., Yan, T., and Wang, X. (2023) Photoluminescence spectroscopy. In *Springer Handbook of Advanced Catalyst Characterization*, 295–321.

27. Lipińska, W., Grochowska, K., Ryl, J., Karczewski, J., Sawczak, M., Coy, E., Mauritz, V., Crisp, R. W. and Siuzdak, K. (2024). Coupling between the photoactivity and CO_2 adsorption on rapidly thermal hydrogenated vs. conventionally annealed copper oxides deposited on TiO_2 nanotubes. *Journal of Materials Science*, **59**, 16947-16962.

28. Hamad, H., Elsenety, M. M., Sadik, W., El-Demerdash, A. G., Nashed, A., Mostafa, A., and Elyamny, S. (2022). The superior photocatalytic performance and DFT insights of S-scheme $CuO@TiO_2$ heterojunction composites for simultaneous degradation of organics. *Scientific Reports*, **12**, 2217.

29. Gnanasekaran, L., Pachaiappan, R., Kumar, P. S., Hoang, T. K., Rajendran, S., Durgalakshmi, D., Soto-Moscoso, M., Cornejo-Ponce, L., and Gracia, F. (2021). p-CuO/n-TiO_2 heterojunction for 4-chlorophenol degradation. *Environmental Pollution*, **287**, 117304.

30. Ahamed, T., Ghosh, A., Show, B., and Mondal, A. (2020). N-TiO_2/p-CuO thin-film heterojunction for dye degradation. *Journal of Materials Science: Materials in Electronics*, **31**, 16616–16633.

31. Ravishankar, T., Vaz, O., and Teixeira, S. (2020). Effects of surfactant on CuO/TiO_2 nanocomposite photocatalysis. *New Journal of Chemistry*, **44**, 1888–1904.

32. Pour, S., Tavangar, R., Namdar, H., Esfandiari, N., and Khorashadizade, E. (2024) Hydrogenated TiO_2 nanotubes modified with Cu/CuO for PEC water splitting. *Journal of Photochemistry and Photobiology A*, **452**, 115586.

33. Hajipour, P., Eslami, A., Bahrami, A., Hosseini-Abari, A., Saber, F. Y., Mohammadi, R., and Mehr, M. Y. (2021) CuO-modified TiO_2 nanoparticles for antibacterial applications. *Ceramics International*, **47**, 33875–33885.

34. Saroha, J., Semalti, P., Tanwar, P., Kumar, M., and Sharma, S. N. (2024) Photocatalytic behaviour of Ag–TiO_2 nanocomposites. *Journal of Applied Physics*, **136**, 055001.

35. Abbas, M. (2021). Adsorption and photocatalysis of direct red 80 using TiO_2. *Journal of Chemical Research*, **45**, 694–701.